immunofluorescence before and after γ-irradiation. The formation of Nbs1 and 53BP1 foci was impaired in H2AX$^{-/-}$ cells, both in the absence and presence of irradiation (Fig. 5, A and B). A few Brca1 foci were present in activated B cells, both in wild-type and H2AX$^{-/-}$ cultures (Fig. 5C); however, irradiation-induced Brca1 foci formed only in wild-type B cells (Fig. 5C). In contrast to the above repair factors, Rad51 formed irradiation-induced foci both in wild-type and H2AX$^{-/-}$ cells (Fig. 5D). Thus, H2AX is required for irradiation-induced Nbs1, 53bp1, and Brca1 focus formation, but not for the assembly of Rad51 foci.

By in situ fractionation, it has been demonstrated that the Mre11 complex colocalizes with proliferating cell nuclear antigen (PCNA) at replication forks during the S phase of the cell cycle (*33*). We used a similar technique to assess whether Nbs1 localization to replication sites was H2AX dependent. The pattern of Nbs1 and PCNA staining in H2AX$^{-/-}$ cells was identical to that observed in wild-type cells (Fig. 5E). Thus, although H2AX is required for irradiation-induced Nbs1 foci, it is not essential for the localization of Nbs1 to sites of replication.

The maintenance of genomic integrity requires the coordinated regulation of DNA replication, DNA-damage cell-cycle checkpoints, and DNA repair. Nbs1 and Brca1 are essential for irradiation-induced S and $G_2$-M cell cycle checkpoints and embryonic viability in mice (*18, 34*). Therefore, the relatively mild phenotype incurred by loss of H2AX is surprising. Our data indicate that there are at least two pathways for Nbs1 recruitment to DNA. In the case of irradiation, H2AX is essential for Nbs1, Brca1, and 53bp1 focus formation, whereas it is not essential for Nbs1 recruitment to sites of DNA replication. The finding that cell-cycle checkpoints are grossly intact in H2AX$^{-/-}$ cells indicates that DNA-damage sensors can detect genome-destabilizing lesions and signal downstream effectors such as Nbs1, Chk2, p53, and Brca1. Nevertheless, loss of H2AX leads to increased chromosomal abnormalities, deficiencies in gene targeting, and radiation sensitivity. We propose that DNA repair proceeds less efficiently in the absence of H2AX and its associated foci.

**References and Notes**


1. C. Redon *et al.*, *Curr. Opin. Genet. Dev.* **12**, 162 (2002).
2. E. P. Rogakou, D. R. Pilch, A. H. Orr, V. S. Ivanova, W. M. Bonner, *J. Biol. Chem.* **273**, 5858 (1998).
3. E. P. Rogakou, C. Boon, C. Redon, W. M. Bonner, *J. Cell Biol.* **146**, 905 (1999).
4. H. T. Chen *et al.*, *Science* **290**, 1962 (2000).
5. S. Petersen *et al.*, *Nature* **414**, 660 (2001).
6. S. K. Mahadevaiah *et al.*, *Nature Genet.* **27**, 271 (2001).
7. T. T. Paull *et al.*, *Curr. Biol.* **10**, 886 (2000).
8. Supplementary methods and figures are available on *Science* Online at www.sciencemag.org/cgi/content/full/1069398/DC1.
9. A. Celeste *et al.*, unpublished observations.
10. C. Barlow *et al.*, *Cell* **86**, 159 (1996).
11. A. Elson *et al.*, *Proc. Natl. Acad. Sci. U.S.A.* **93**, 13084 (1996).
12. Y. Xu *et al.*, *Genes Dev.* **10**, 2411 (1996).
13. Y. Gu *et al.*, *Immunity* **7** (1997).
14. A. Nussenzweig *et al.*, *Nature* **382**, 551 (1996).
15. M. J. Difilippantonio *et al.*, *Nature* **404**, 510 (2000).
16. Z. E. Karanjawala, U. Grawunder, C. L. Hsieh, M. R. Lieber, *Curr. Biol.* **9**, 1501 (1999).
17. M. Liyanage *et al.*, *Blood* **96**, 1940 (2000).
18. D. C. van Gent, J. H. Hoeijmakers, R. Kanaar, *Nat. Rev. Genet.* **2**, 196 (2001).
19. A. Nussenzweig, K. Sokol, P. Burgman, L. Li, G. C. Li, *Proc. Natl. Acad. Sci. U.S.A.* **94**, 13588 (1997).
20. J. Essers *et al.*, *EMBO J.* **19**, 1703 (2000).
21. Y. Gao *et al.*, *Nature* **404**, 897 (2000).
22. D. O. Ferguson *et al.*, *Proc. Natl. Acad. Sci. U.S.A.* **97**, 6630 (2000).
23. E. Sonoda *et al.*, *EMBO J.* **17**, 598 (1998).
24. J. A. Downs, N. F. Lowndes, S. P. Jackson, *Nature* **408**, 1001 (2000).
25. R. Casellas *et al.*, *EMBO J.* **17**, 2404 (1998).
26. J. P. Manis *et al.*, *J. Exp. Med.* **187**, 2081 (1998).
27. A. Rolink, F. Melchers, J. Andersson, *Immunity* **5**, 319 (1996).
28. M. R. Ehrenstein, M. S. Neuberger, *EMBO J.* **18**, 3484 (1999).
29. C. E. Schrader, W. Edelmann, R. Kucherlapati, J. Stavnezer, *J. Exp. Med.* **190**, 323 (1999).
30. R. Shroff and M. Lichten, personal communication.
31. E. Sonoda *et al.*, *Mol. Cell. Biol.* **19**, 5166 (1999).
32. J. Essers *et al.*, *Cell* **89**, 195 (1997).
33. R. S. Maser *et al.*, *Mol. Cell. Biol.* **21**, 6006 (2001).
34. J. Zhu, S. Petersen, L. Tessarollo, A. Nussenzweig, *Curr. Biol.* **11**, 105 (2001).



35. We thank J. Chen, S. Ganesan, D. Livingston, P. Moens, B. Spyropoulos, and C. Heyting for antisera; T. Ried, X. Tai, J. Zhu, S. Kerns, S. Gonzalez, K. Hathcock, and M. Krulack for assistance; R. Kanaar for gene-targeting constructs; R. Schroff and M. Lichten for sharing unpublished data; and A. Singer and M. Lichten for comments on the manuscript and helpful discussions. This work was supported in part by grants from the NIH and the Leukemia Society (M.C.N.). M.C.N. is a Howard Hughes Medical Institute investigator.

27 December 2001; accepted 22 March 2002
Published online 4 April 2002;
10.1126/science.1069398
Include this information when citing this paper.


# Contact-Dependent Demyelination by *Mycobacterium leprae* in the Absence of Immune Cells


**Anura Rambukkana,[1]* George Zanazzi,[2] Nikos Tapinos,[1] James L. Salzer[2]**



**Demyelination results in severe disability in many neurodegenerative diseases and nervous system infections, and it is typically mediated by inflammatory responses. *Mycobacterium leprae*, the causative organism of leprosy, induced rapid demyelination by a contact-dependent mechanism in the absence of immune cells in an in vitro nerve tissue culture model and in *Rag1*-knockout (*Rag1*$^{-/-}$) mice, which lack mature B and T lymphocytes. Myelinated Schwann cells were resistant to *M. leprae* invasion but undergo demyelination upon bacterial attachment, whereas nonmyelinated Schwann cells harbor intracellular *M. leprae* in large numbers. During *M. leprae*–induced demyelination, Schwann cells proliferate significantly both in vitro and in vivo and generate a more nonmyelinated phenotype, thereby securing the intracellular niche for *M. leprae*.**


Demyelination is one of the central pathologic conditions that ultimately lead to prolonged neurologic disability in many neurodegenerative diseases (*1*). The process of demyelination involves multiple factors (*2*). Although inflammatory responses seem to be needed for the complete manifestation of pathologic conditions of demyelination and associated neurological symptoms (*1, 3*), virtually nothing is known about the mechanisms involved in early events of such neurological injury. One of the classic examples of infectious neurodegenerative diseases of the peripheral nervous system (PNS) is leprosy, which is caused by the obligate intracellular bacterium *Mycobacterium leprae* (*4*) and is a leading cause of nontraumatic neuropathies in the world (*3*). Demyelination is a common pathologic feature in the nerve damage in leprosy (*5–8*) and is likely to substantially contribute to the neurologic disability in these patients. The nerve damage in leprosy is widely thought to be secondary to the


[1]Laboratory of Bacterial Pathogenesis and Immunology, The Rockefeller University, New York, NY 10021, USA. [2]Departments of Cell Biology and Neurology, New York University Medical Center, New York, NY 10016, USA.

*To whom correspondence should be addressed. E-mail: rambuka@mail.rockefeller.edu

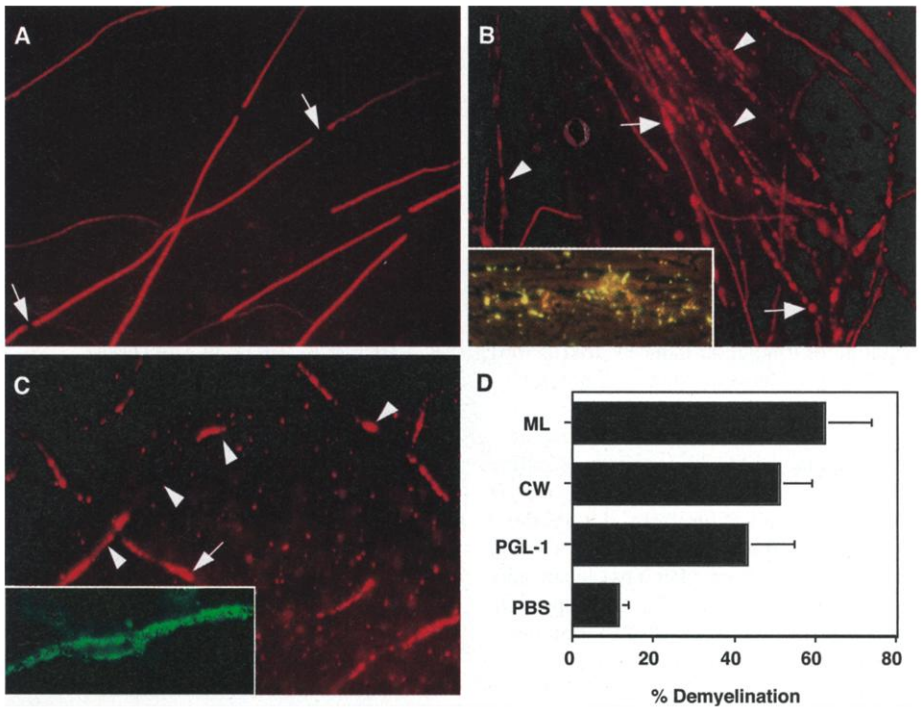


**Fig. 1.** Attachment of *M. leprae* and its cell-wall components to Schwann cell–axon units in vitro induces striking demyelination. (**A**) Control immunofluorescence micrograph showing a Schwann cell–DRG neuron coculture that had myelinated for 3 weeks and was labeled with monoclonal antibody (mAb) against myelin basic protein (MBP), which represents the compact myelin. Note the intact myelin segments, one of which is demarcated by arrows that denote the nodes of Ranvier. (**B**) *M. leprae* induce significant demyelination upon attachment. Cocultures were first incubated for 1 hour with *M. leprae* to attach to Schwann cell–axon units and then further incubated for another 24 hours, fixed, and labeled with MBP-specific antibody. Inset shows the attached *M. leprae* (green notes) to nerve fibers in similar cultures as visualized by acid-fast labeling (*13*). Note the demyelinating nerve fibers (arrowheads) with characteristic myelin ovoids (arrows) as compared with intact myelin segments in controls. (**C**) PGL-1 of the *M. leprae* cell wall is sufficient to induce significant demyelination. Myelinated cocultures were treated with purified native PGL-1 as in (B). After 24 hours, PGL-1 causes significant demyelination, which is similar to that of whole *M. leprae* (B). Inset shows the bound PGL-1 (green) to a myelinated nerve fiber after 1 hour of incubation and detected by anti-PGL-1 mAb. Demyelinated fibers indicated by the arrowheads and the myelin ovoids are shown by the arrows. Also shown are myelin debris labeled with MBP-specific antibody as red dots. (**D**) Quantification of in vitro demyelination induced by *M. leprae* (ML), the total cell wall (CW), and purified native PGL-1 (PGL-1) as compared with controls (PBS). Fibers were classified as demyelinated if the myelin sheath was crenated or fragmented and the percentage of demyelination was quantified from two to three separate experiments.

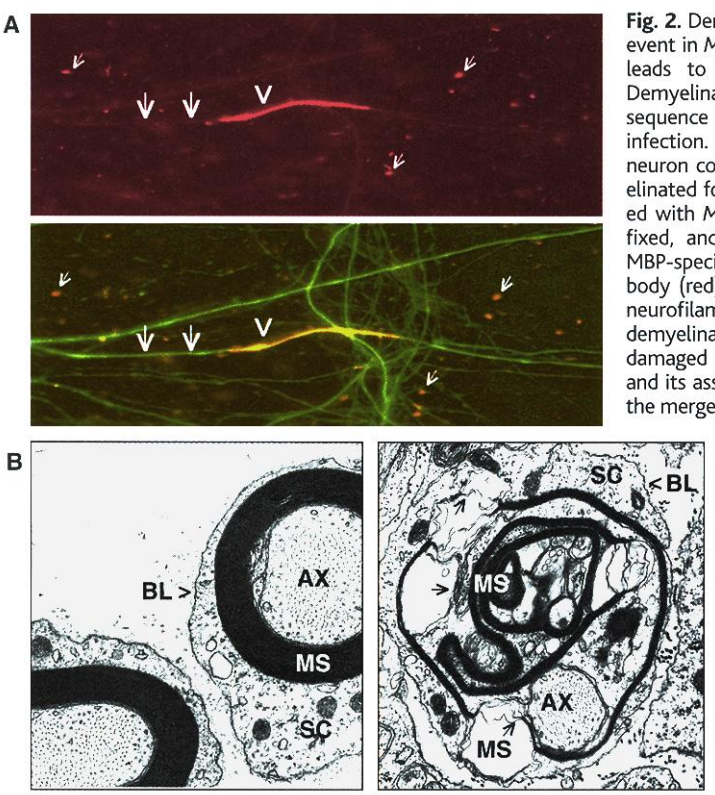


**Fig. 2.** Demyelination is an early event in *M. leprae* infection that leads to axonal damage. (**A**) Demyelination is an initial consequence of in vitro *M. leprae* infection. Schwann cell–DRG neuron cocultures that had myelinated for 3 weeks were treated with *M. leprae* for 12 hours, fixed, and double-labeled with MBP-specific polyclonal antibody (red) and an mAb against neurofilament mAb (green). A demyelinated nerve fiber with a damaged myelin sheath (top) and its associated intact axon in the merged image (bottom; MBP is in red/orange and neurofilament is in green) are shown by the arrows. The arrowheads denote the Schwann cell nucleus of the demyelinated fiber. Also note the numerous myelin debris (red/orange particles), which are indicated by the small arrows. (**B**) Axonal degeneration is a late event of *M. leprae* infection. Electron micrographs showing the ultrastructure of myelinated Schwann cell (SC)–axon (AX) units with surrounding basal lamina (BL) of cocultures that are untreated (left) and treated with *M. leprae* for 72 hours (right). Note the splitting of the myelin lamellae (arrows), the disorganized myelin sheath (MS), and the displaced degenerating axon in *M. leprae*–infected cultures as compared with controls.

immune response against *M. leprae* itself (*3*, *4*, *8*). Because Schwann cells in the PNS provide a privileged site for *M. leprae* that eludes surveillance by the host immune cells, the early induction of nerve damage may not be associated with immune responses (*9*). To test this hypothesis and to gain insight into the functional consequences of early *M. leprae* interaction with peripheral nerves, we used a well-characterized myelinating Schwann cell–dorsal root ganglion (DRG) neuron coculture system (*10*) and mice with null mutation for the recombination-activating gene 1 ($Rag1^{-/-}$), which lack mature T and B lymphocytes (*11*), as in vitro and in vivo models, respectively.

In Schwann cell–DRG neuron cocultures, *M. leprae* (*12*) avidly bound to both myelinating and nonmyelinating Schwann cell–axon units after 1 hour of inoculation [Fig. 1B, inset (*13*)]. We studied the functional consequences of this binding (*14*) on individual Schwann cell phenotypes. In myelinating Schwann cells, *M. leprae* induces significant demyelination 24 hours after bacterial attachment in a dose-dependent manner, whereas in nonmyelinating Schwann cells, bacterial invasion in large numbers is the most conspicuous feature. The induction of demyelination by *M. leprae* was rapid and was observed as early as 24 hours after infection (Fig. 1, B and D) without any signs of apoptosis (*15*) or

cytopathic effects to Schwann cells (*16*), suggesting that *M. leprae*–induced demyelination does not result from apoptosis or toxic effects. Demyelination was found over long lengths of the nerve or in short sporadic segments as compared with cultures treated with phosphate-buffered saline (PBS) alone (Fig. 1, A and B). Electron microscopic analysis further showed disrupted myelin sheaths and the separation of lamellae with wide spaces as compared with intact myelin sheaths in controls (Fig. 2B). The most distinctive feature is the formation of myelin ovoids (Fig. 1B), which are characteristics of myelin pathology (*17*, *18*). Because the axons remain intact in most of these demyelinating fibers at early time points (Fig. 2A), this condition resembles classic segmental demyelination (*17*, *18*), which is also common in leprosy patients (*3*, *5*–*7*). Experiments performed in parallel with *Mycobacterium smegmatis*, a related species that does not cause neuropathy, showed no significant demyelination (<20%) (*16*).

Viability of *M. leprae* is not required for its ability to induce demyelination in vitro, because γ-irradiated *M. leprae* and the *M. leprae* cell-wall fraction alone (*19*) were as effective as live bacteria (Fig. 1D). This suggests that the components of the *M. leprae* cell wall have the capacity to induce demyelination during early infection. Prominent among the biologically active components of the *M. leprae* cell wall is *M. leprae*–specific phenolic glycolipid-1 (PGL-1) (*19*–*22*), which has recently been implicated for the neural predilection of *M. leprae* (*21*). Although PGL-1 represents >2% of the bacterial mass, little is known about its biological functions (*20*). Here we show that the binding of native PGL-1 (*19*) to myelinating nerve fibers [Fig. 1C, inset; (*21*)] results in demyelination in a dose- and time-dependent manner (Fig. 1, C and D). Because the pattern of PGL-1–induced demyelination resembles that of whole *M. leprae* (Fig. 1, B and C), we propose that the PGL-1 is a crucial molecule in the *M. leprae* cell wall that is directly involved in the neuropathogenesis of leprosy. We also excluded the possibility that demyelination, induced by the *M. leprae* cell-wall or PGL-1 preparations, was caused by contamination with lipopolysaccharide or other endotoxins (*14*).

A time-course analysis showed that demyelination is an initial event that is followed by axonal damage during *M. leprae* infection. Although axons remain intact in early infection (Fig. 2A), *M. leprae*–treated cultures began to exhibit substantial axonal degeneration in addition to the myelin damage after 72 hours (Fig. 2B). However, no bacteria were found in axons (*16*). Because our in vitro culture model is completely devoid of immune cells, but only comprised of Schwann cells and neurons, we conclude that such in vitro induction of demyelination and axonal degeneration by *M. leprae* is mediated by a nonimmune mechanism(s).

To test this in vivo, we used *Rag1*$^{-/-}$ mice, which lack mature T and B lymphocytes and thus are incapable of mounting adaptive immune responses against pathogens (*11*). Although null mutation of the *Rag1* gene causes severe deficiency in the immune system, the nervous system of these mice is intact (*11*). In the PNS, sciatic nerves of *Rag1*$^{-/-}$ mice show normal, thick and compact myelin as in wild type [Fig. 3, A and C; (*23*)]. Intraneural administration of either viable or dead *M. leprae* or the whole cell-wall fraction to sciatic nerves of *Rag1*$^{-/-}$ mice (*24*) produced significant demyelination ($P < 0.0005$) in varying degrees as compared with that in the mice injected with PBS (Fig. 3, A to D). Myelin breakdown in various stages was seen in all the fascicles of *M. leprae*–infected nerves with widely separated myelin lamellae (Fig. 3, B and D). Semithin sections of sciatic nerves and the corresponding electron microscopic analysis revealed that demyelination in infected nerves was time-dependent and quite dramatic after 72 hours (Fig. 3, B and D). Labeling of teased fibers prepared from infected and control sciatic nerves with antibody to myelin-specific P0 protein further confirmed demyelinated fibers and characteristic myelin ovoids in *M. leprae*–infected nerves (Fig. 3, E and F). As in *Rag1*$^{-/-}$ mice, *M. leprae* injection to sciatic nerves of wild-type C57BL/6 (B6) mice also caused considerable demyelination as early as 24 hours (*16*). Because inflammatory cells are unlikely to be recruited at such an early stage (24 hours), we suggest that demyelination in wild-type mice in early infection is also caused by a nonimmune mechanism(s). Our finding that demyelination can be induced by dead *M. leprae* or bacterial cell wall alone both in vitro and in vivo may provide new insights into the underlying causes for continuing neurological injuries in patients who have been cured of leprosy (bacteriological cure) after multidrug therapy (*25*). It is likely that such nerve damage may be associated with dead *M. leprae* or residual cell-wall components, such as PGL-1, retained in nerve tissues in treated leprosy patients (*26*).

In demyelinating diseases, inflammation and/or immune responses are thought to be

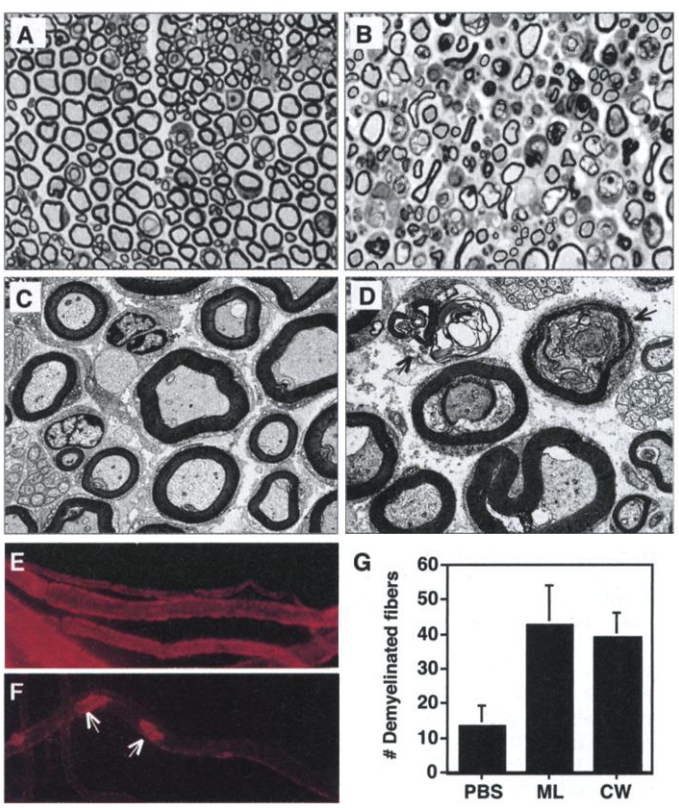


**Fig. 3.** In vivo induction of demyelination in early *M. leprae* infection does not require inflammatory and/or immune response. (**A** and **B**) Methylene blue–stained semithin transverse sections of sciatic nerves of *Rag1*$^{-/-}$ knockout mice 72 hours after intraneural injection of PBS (A), and viable *M. leprae* (B). Note the degenerated myelinated fibers in *M. leprae*–treated nerves. (**C** and **D**) Electron microscopy analysis of corresponding sections as in (A) reveals normal compact myelinated fibers with intact axons in the PBS-injected nerves (C), whereas the nerves injected with viable *M. leprae* (D) show varying degrees of demyelination and axonal damage. The arrows indicate the fibers with extensive demyelination. Also note the collagen deposition and increased endoneural space in infected nerves. (**E** and **F**) Demyelination in teased sciatic nerve fibers. Teased fiber preparation from sciatic nerves injected with PBS (E) and *M. leprae* (F) were labeled with P0-specific antibody. Note the demyelination and formation of myelin ovoids (arrows) as confirmed by antibody to myelin-specific P0 protein. (**G**) Quantification of in vivo demyelination revealed a significant difference ($P < 0.0005$) in the number of demyelinated fibers in the sciatic nerves infected with viable *M. leprae* (ML) and the cell-wall (CW) fraction as compared with those treated with PBS.

the cause for the myelin damage, in which macrophages, T lymphocytes, and antibodies play the crucial roles (*1*, *2*, *4*). However, much less is known about alternative mechanisms for myelin damage. In *M. leprae*–induced demyelination, we found that there was no evidence of macrophage infiltration, as the number of CD68-positive macrophages was rare in the endoneurium of the sciatic nerves of infected *Rag1*$^{-/-}$ mice (*16*). Because *Rag1*$^{-/-}$ mice are also devoid of functional T and B cells (*11*), we conclude that the demyelination induced by *M. leprae* in vivo is not the result of antibody-mediated phenomena or macrophage- or T cell–mediated inflammatory processes. Because these pathological conditions induced by *M. leprae* in both in vivo and in vitro models resemble neuropathies in human leprosy (*3*, *7*), they may represent an early phase of nerve damage in patients with other neurodegenerative diseases. One possible mechanism for such non-immune-mediated demyelination and/or nerve injury would be the perturbation of homeostasis of the neural microenvironment and signaling network by *M. leprae* infection.

An important consequence of *M. leprae* attachment to the Schwann cell–axon units is bacterial invasion. Molecular dissection of *M. leprae* attachment and early invasion in animal models has been difficult, however, mainly owing to the failure of localization of *M. leprae* within Schwann cells for as yet unknown reasons (*27*). Although this was also the case in *Rag1*$^{-/-}$ mice described in the present study (*16*), we could localize significant numbers of *M. leprae* in close proximity to myelinated and nonmyelinated Schwann cells within the endoneurium, and some bacteria were found attached to myelinated Schwann cells (Fig. 4C).

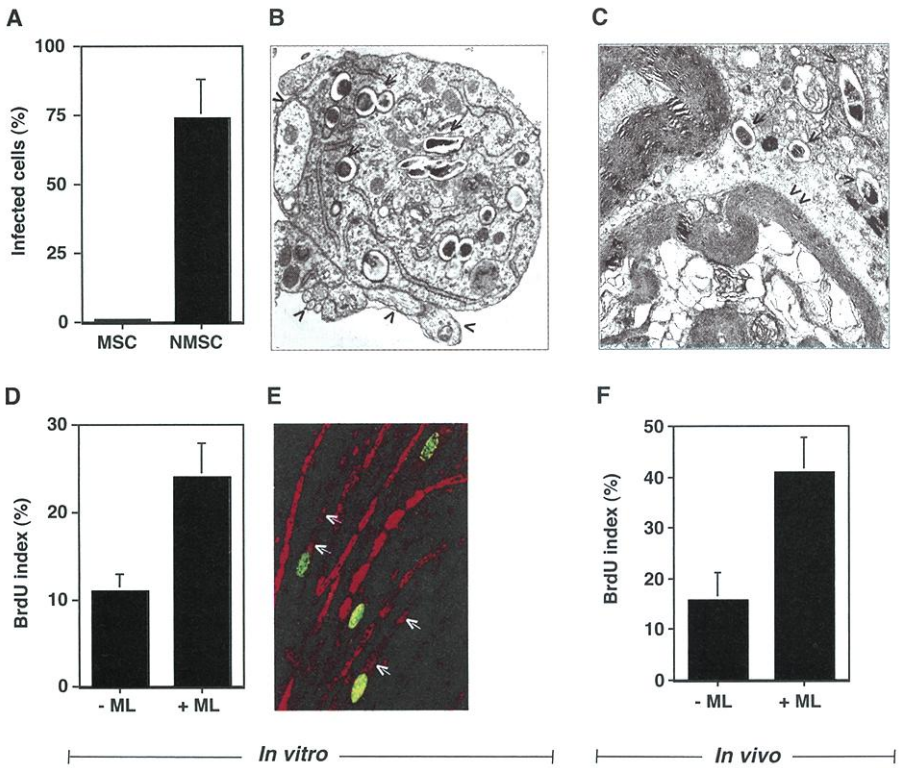


**Fig. 4.** Distinct functional consequences of nonmyelinated and myelinated Schwann cells in response to *M. leprae* infection in vitro and in vivo; bacterial invasion, demyelination, and Schwann cell proliferation. (**A** and **B**) Nonmyelinated Schwann cells (NMSC) are preferentially invaded by *M. leprae*, whereas myelinated Schwann cells (MSC) are resistant to bacterial invasion but undergo demyelination (see Fig. 1). (A) Quantification of nonmyelinated and myelinated Schwann cells infected with *M. leprae* in vitro. (B) Intracellular *M. leprae* (arrows) were found exclusively in nonmyelinated Schwann cells in high numbers. Axons in nonmyelinated Schwann cells are normal (arrowheads) in spite of the numerous bacteria. (**C**) Representative electron micrograph of sciatic nerve of *Rag1*$^{-/-}$ mice 72 hours after infection showing extracellular *M. leprae* (arrows) either attached to or close to myelinated Schwann cells, one of which is shown with extensive demyelination (double arrowheads). (**D** to **F**) In vitro and in vivo proliferation of Schwann cells in *M. leprae*–infected Schwann cell–neuron cocultures and sciatic nerves of *Rag1*$^{-/-}$ mice that are undergoing demyelination. Quantification of 5-bromo-2′-deoxyuridine (BrdU)-positive cells in cocultures (D) and in teased fiber preparations from sciatic nerves of *Rag1*$^{-/-}$ mice (F) reveals that *M. leprae* (+ML) induce a statistically significant increase in Schwann cell proliferation ($P < 0.05$ and $P < 0.005$ in vitro and in vivo, respectively). (E) Representative confocal micrograph showing demyelinated fibers associated with Schwann cell proliferation in vitro as detected by double-labeling with BrdU-specific antibody (green) and MBP-specific mAb (red). The arrows denote the demyelinated fibers (red) with proliferating Schwann cell nuclei (green).

In contrast, the nerve culture model was found to be suitable for *M. leprae* invasion studies, because this in vitro model mimics the preferential localization of *M. leprae* to nonmyelinated Schwann cells as in patients with lepromatous leprosy (*6*, *7*) (described below). We have therefore focused our efforts on this in vitro model of *M. leprae* invasion.

Analyzing the events of *M. leprae* invasion in myelinated versus nonmyelinated phenotypes in in vitro cultures (*28*) showed striking differences. The most consistent finding in myelinated Schwann cells is their resistance to *M. leprae* invasion even after 72 hours (Fig. 4A), although at that time point *M. leprae* induces significant demyelination and axonal degeneration in this phenotype (Fig. 2B). This clearly indicates that *M. leprae* invasion is not necessary to cause demyelination, but the bacterial attachment alone is sufficient to induce this nerve pathology via a contact-dependent mechanism(s). This also seems to be the case in *Rag1*$^{-/-}$ mice infected with *M. leprae*, because some bacteria were found attached to or in the vicinity of the myelinated Schwann cells that are undergoing demyelination in vivo (Fig. 4C).

In contrast to myelinated Schwann cells, nonmyelinated Schwann cells are highly susceptible to *M. leprae* invasion in vitro, with intracellular bacteria found in the majority of nonmyelinated cells (>75%) in varying degrees (that is, 1 to 30 bacteria per cell; Fig. 4, A and B). This is also the case in human leprosy, where intracellular *M. leprae* are frequently seen in nonmyelinated Schwann cells (70 to 80%) in the early stage, but bacilli are rarely seen in myelinated Schwann cells (~4%) even in advanced lepromatous patients with high bacterial load (*6*, *7*). This susceptibility of nonmyelinated Schwann cells to *M. leprae* invasion may provide this bacterium with a clear advantage for its intracellular survival within the PNS. *M. leprae*–induced demyelination and axonal damage in vitro and in vivo resemble peripheral nerve injury such as in Wallerian degeneration, where Schwann cells rapidly proliferate to promote the regeneration of injured nerves (*29*). Strikingly, Schwann cells in *M. leprae*–infected cocultures and sciatic nerves of *Rag1*$^{-/-}$ mice proliferate (*30*) significantly ($P < 0.05$ and $P < 0.005$, respectively) after 72 hours (Fig. 4, D to F), at which point myelinated fibers both in vitro and in vivo have undergone substantial demyelination and axonal degeneration (Figs. 2B and 3). On the basis of these findings, we propose that *M. leprae*–induced nerve injury contributes to Schwann cell proliferation, as in other nerve injury responses (*29*), and, thereby, increases the number of nonmyelinating Schwann cells in the early phase of the infectious process. Because *M. leprae* is an obligate intracellular bacterium, it must invade its preferred nonmyelinating phenotypes in order to survive within the PNS.

However, as the infection progresses and bacteria undergo unrestrained multiplication, the availability of nonmyelinating Schwann cells becomes a limiting factor. To avoid such a situation, leprosy bacilli may induce demyelination and axonal damage as an effective strategy to increase the number of nonmyelinating Schwann cells so that a sufficient intracellular niche is available for bacterial survival. Because myelinated Schwann cells do not serve as an intracellular niche for *M. leprae*, we propose that *M. leprae* propagates a nonmyelinating phenotype by inducing demyelination and nerve injury in myelinated Schwann cells in the early phase of infection, a novel bacterial survival strategy in the nervous system.

### References and Notes


1. S. G. Waxman, *N. Engl. J. Med.* **338**, 323 (1998).
2. D. M. Wingerchuk, C. F. Lucchinetti, J. H. Noseworthy, *Lab Invest.* **81**, 263 (2001).
3. P.C. Johnson, in *Textbook of Neuropathology*, R. L. Davis and D. M. Robertson, Eds. (Williams and Wilkins, Baltimore, MD, 3rd ed., 1997), pp. 1233–1323.
4. G. L. Stoner, *Lancet* **10**, 994 (1979).
5. J. M. Jacobs, V. P. Shetty, N. H. Antia, *J. Neurol. Sci.* **79**, 301 (1987).
6. V. P. Shetty, L. N. Mehta, P. F. Irani, N. H. Antia, *Lep. India* **52**, 5 (1980).
7. V. P. Shetty, J. M. Jacobs, N. H. Antia, *J. Neurol. Sci.* **88**, 115 (1988).
8. C. K. Job, *Int. J. Lepr.* **57**, 532 (1989).
9. A. Rambukkana, *Curr. Opin. Microbiol.* **4**, 21 (2001).
10. S. Einheber, T. A. Milner, F. Giancotti, J. L. Salzer, *J. Cell Biol.* **123**, 1223 (1993).
11. P. Mombaerts *et al.*, *Cell* **68**, 869 (1992).
12. In vivo grown *M. leprae* were purified from armadillos and nude mice and provided by P. J. Brennan (Colorado State Univ., Fort Collins, CO) and J. Krahenbuhl (Hansen's Disease Center, Baton Rouge, LA), respectively.
13. A. Rambukkana, J. L. Salzer, P. D. Yurchenco, E. I. Tuomanen, *Cell* **88**, 811 (1997).
14. Details of the experimental procedures for in vitro infection (*14*) and evidence regarding lack of contamination are available on *Science* Online at www.sciencemag.org/cgi/content/full/296/5569/927/DC1.
15. Cells undergoing apoptosis in *M. leprae*–treated and control cultures were determined by terminal deoxynucleotidyl transferase (TdT)-mediated dUTP nick end-labeling (TUNEL) assay kit according to the manufacturer's instructions (Roche Molecular Biochemicals).
16. A. Rambukkana, unpublished data.
17. Ramon y Cajal, *Degeneration and Regeneration of the Nervous System* (Oxford Univ. Press, Oxford, UK, 1928).
18. D. E. Pleasure, J. Towfighi, *Arch. Neurol.* **26**, 289 (1972).
19. S. W. Hunter, P. J. Brennan, *J. Bacteriol.* **147**, 728 (1981).
20. P. J. Brennan, *Rev. Infect. Dis.* **11** (Suppl. 2), S420 (1989).
21. V. Ng *et al.*, *Cell* **103**, 511 (2000).
22. Native PGL-1 was purified from armadillo tissue (*19*) and provided by P. J. Brennan.
23. C. D. Schmid *et al.*, *J. Neurosci.* **20**, 729 (2000).
24. Details of the experimental procedures for in vivo infection are available on *Science* Online at www.sciencemag.org/cgi/content/full/296/5569/927/DC1.
25. R. Curtiss III *et al.*, *Lepr. Rev.* **72**, 8 (2001).
26. V. P. Shetty, M. W. Uplekar, N. H. Antia, *Acta Neuropathol.* **88**, 300 (1994).
27. V. P. Shetty, *Int. J. Lepr.* **61**, 70 (1993).
28. Details of the experimental procedures for *M. leprae* invasion in vitro are available on *Science* Online at www.sciencemag.org/cgi/content/full/296/5569/927/DC1.
29. S. S. Scherer, J. L. Salzer, in *Glial Cell Development*, K. R. Jessen and W. D. Richardson, Eds. (Bios Scientific Publishers, London, 1996), pp. 165–196.
30. Details of the experimental procedures for Schwann cell proliferation are available on *Science* Online at www.sciencemag.org/cgi/content/full/296/5569/927/DC1.


31. We thank V. A. Fischetti and E. C. Gotschlich for continuing support and encouragement, P. J. Brennan and J. Krahenbuhl for providing *M. leprae* and its components through NIAID/NIH contract, and H. Shio for excellent electron microscopy analyses. This work was funded by R01 grants from the NIH/NIAID (to A.R.), NINDS (to J.L.S.), and the UNDP/World Bank/WHO Special Program for Research in Tropical Diseases (to A.R.).

11 November 2001; accepted 6 February 2002


# Enhanced and Delayed Stress-Induced Alcohol Drinking in Mice Lacking Functional CRH1 Receptors


**Inge Sillaber,[1]*† Gerhard Rammes,[1]* Stephan Zimmermann,[1] Beatrice Mahal,[1] Walter Zieglgänsberger,[1] Wolfgang Wurst,[1,2] Florian Holsboer,[1] Rainer Spanagel[1,3]**



**There is a relation between stress and alcohol drinking. We show that the corticotropin-releasing hormone (CRH) system that mediates endocrine and behavioral responses to stress plays a role in the control of long-term alcohol drinking. In mice lacking a functional CRH1 receptor, stress leads to enhanced and progressively increasing alcohol intake. The effect of repeated stress on alcohol drinking behavior appeared with a delay and persisted throughout life. It was associated with an up-regulation of the *N*-methyl-D-aspartate receptor subunit NR2B. Alterations in the CRH1 receptor gene and adaptional changes in NR2B subunits may constitute a genetic risk factor for stress-induced alcohol drinking and alcoholism.**


Alcoholism is a multifactorial disorder in which the environment interacts with genetic predisposition to produce the final level of risk (*1*, *2*). Stressful life events and maladaptive responses to stress influence alcohol drinking and relapse behavior (*3*–*6*). Although the relation between stress and alcohol drinking in humans (*3*, *4*) and laboratory animals (*5*, *6*) is complex, it is known that in some individuals alcohol drinking is an attempt to cope with stress. Stress-induced alcohol drinking and relapse behavior apparently have a significant genetic component (*7*, *8*), but molecular and cellular mechanisms underlying stress-induced alcohol drinking and relapse behavior are still obscure. Recent studies have implicated the CRH system and the glutamatergic system in these processes (*9*, *10*).

CRH regulates endocrine responses to stress (*11*) and mediates stress-related behavioral responses by means of extrahypothalamic sites (*12*). The CRH signal is transmitted by two types of receptors, termed the CRH1 and CRH2 receptors, which differ in their pharmacology and expression pattern in the brain (*13*, *14*). Dysregulation in the CRH/CRH1-receptor system has been attributed to a variety of stress-related psychiatric disorders, including alcoholism (*9*). Mice lacking a functional CRH1 receptor (*Crhr1*$^{-/-}$) (*15*) represent a useful animal model to address the question of whether a dysfunctional CRH/CRH1-receptor system influences individual vulnerability for alcohol drinking, under basal and stress conditions, and whether long-term alcohol self-administration is influenced by this mutation.

Before studying alcohol drinking in *Crhr1*$^{-/-}$ mice, we further tested the functional impairment of the CRH1 receptor. *Crhr1*$^{-/-}$ mice that are lacking the G protein–coupling domain show a blunted hormonal stress response (*15*). Extracellular field potential measurements that are exemplary in the CA1 region of the hippocampus were used to document the dysfunctional signal transduction (*16*). In an in vitro prepara-


[1]Max Planck Institute of Psychiatry, Kraepelinstrasse 2-10, 80804 Munich, Germany. [2]National Research Center for Environment and Health, Institute for Mammalian Genetics, Ingolstädter Landstrasse 1, 85764 Munich, Germany. [3]Central Institute of Mental Health, University of Heidelberg, J5, 68159 Mannheim, Germany.

*These authors contributed equally to this work.
†To whom correspondence should be addressed. E-mail: sillaber@mpipsykl.mpg.de